Supplementary Information (SI) for Journal of Materials Chemistry A.

Influence of electrolyte on the photo-charging capability of a ZnO-FTO supercapacitor

Pankaj Singh Chauhan[1*], Mihir Parekh[2*], Santilata Sahoo[1], Sumana Kumar[1], Ayon Das Mohapatra[1], Pragya Sharma[1], Vinod Panwar[1], Apparao M. Rao[2], Abha Misra[1#]

[1]*Department of Instrumentation and Applied Physics, Indian Institute of Science, Bangalore, Karnataka, India 560012*

[2]*Department of Physics & Astronomy, Clemson Nanomaterials Institute, Clemson University, Anderson, SC, USA 29625*

* *Both authors contributed equally*
\# *Corresponding author:* abha@iisc.ac.in

A continuum scale physics-based analytical model for photo-rechargeable supercapacitor

We assume that the thickness of the ZnO-FTO electrode is h_0 (m) and the intensity of UV light is I_0 (W/m^2).

We begin by assuming that the absorptivity of the ZnO-FTO electrode is α (m^{-1}), the frequency of the UV light is ν, and quantum efficiency is 1, and the electrode surface area exposed to incoming radiation is A (m^2). This implies that the electron-hole pair generation rate (per unit volume) G $(m^{-2}s^{-1})$ is given by

$$\frac{I_0(1-\exp(-\alpha h_0))}{h\nu} = G. \qquad 1$$

The electron concentration and hole concentration within the ZnO-FTO electrode are $n_e(t)$ (m^{-2}) and $n_h(t)$ (m^{-2}), respectively, and the current density due to ionic flux within the electrolyte is assumed to be J $\left(A/m^2\right)$, i.e., $J = \sum z_i F N_i$, where N_i is the flux of species *i* within the electrolyte.

For consistency, we always illuminated the negative electrode (even though this study investigated symmetrical supercapacitors) and developed the model described below. This is because illuminating the negative electrode is expected to lead to a higher rise in capacitance than illuminating the positive electrode due to the alignment of the fermi levels of ZnO and FTO.

If light is shone on the negative electrode, then within the negative electrode,

$$\frac{dn_e(t)}{dt} = \frac{J}{e} = G - R - \frac{I}{e}, \qquad 2$$

$$\frac{dn_h(t)}{dt} = G - R,$$

3

where

$$R = k_R n_e n_h$$

4

is the rate of recombination with k_R $(m^2 s^{-1})$ being the recombination rate constant and I (Am^{-2}) is the current density through the external circuit. Moreover, e is absolute value the electronic charge i.e. $e = 1.6E - 19\ C$.

In Eq. 2, the rate of change of electronic concentration in the negative electrode under illumination is equal to the difference between the rate of electron-hole pair generation, recombination rate and the rate of withdrawal of electrons from the electrode (which is equal to the current density in the external circuit (I)). The change in electronic concentration within the electrode further contributes towards the flux of ions within the electrolyte, J. Furthermore, Eq. 2 implies that in the absence of illumination $G = R = 0,\ J = -I$. Thus, galvanostatic conditions without illumination imply $\frac{dJ}{dt} = 0 = \frac{dI}{dt}$.

In Eq. 3, the rate of change of hole concentration within the electrode has been equated to the difference between the electron-hole pair generation rate and the recombination rate. Specifically, we assume that the hole current within the electrode contributes negligibly to the current in the external circuit. This assumption is based on the knowledge of the alignment of fermi levels of ZnO and FTO, which makes it easier for electrons to move and prohibits the holes from moving.

Equation 4 assumes that the recombination reaction follows second-order chemical kinetics (first order with respect to electrons and first order with respect to holes, but overall second order). It must be noted that since Eqs. 2 and 3 both have the same recombination rate R, it implies that defect and interface recombination rates have been assumed to be negligible compared to the radiative recombination rate.

Further, the appearance of a peak in cyclic voltammetry curves can either be ascribed to pseudocapacitor-like behavior, meaning the presence of redox reaction-based charge transfer across the electrode-electrolyte interface, or to mass transfer-limited ionic transport within the electrolyte. The presence of the peaks at higher scan rates (for PVA/KCl gel-based electrolyte under illumination) and their absence at lower scan rates (Figs. S1, and 4c) clearly indicates that these peaks are not due to pseudocapacitive behavior because if the peaks arose due to redox reactions, then they should have been more prominent at lower scan rates such as 10 mV/s, than at the larger scan rates. The model presented below further confirms that the peaks owe their presence to the mass transfer-limited ionic transport within the electrolyte.

For a peak to arise in the cyclic voltammetry curves, at the peak,

$$\frac{dI}{dt} = 0, \tag{5}$$

$$\frac{dI}{dt} = 0 = -k_R e\left(n_h \frac{dn_e}{dt} + n_e \frac{dn_h}{dt}\right) - \frac{dJ}{dt}, \tag{6}$$

Here, $\frac{dG}{dt} = 0$ because G is expected to remain constant as long as the illumination intensity and material properties do not change with time. Using Eqs. 2, 3, and the fact that for mass-transported limited ionic flux, $J = J_{max} = k_1$ and $\frac{dJ}{dt} = 0$ gives

$$n_e = \frac{k_1 t}{e} + k_2, \tag{7}$$

and

$$\frac{dn_h}{dt} = k_3 - k_R(k_1 t/e + k_2)n_h, \tag{8}$$

where $k_3 = G$. This gives

$$n_h(t = t_{peak}) = \frac{k_3(k_1 t_{peak}/e + k_2)}{\left(-k_1/e + k_R\left(k_1 t_{peak}/e + k_2\right)^2\right)}, \tag{9}$$

where t_{peak} is the time at which peak current is observed. Using Eqs. 7, 8, 9, $J = J_{max} = k_1$, and $k_3 = G$ in Eq. 2 (for mass transport limited ionic flux) gives

$$\frac{I_{peak}}{e} = k_3 - \frac{k_1}{e} - \frac{k_3\left(\frac{k_1 t_{peak}}{e} + k_2\right)^2}{\frac{-k_1}{ek_R} + \left(\frac{k_1 t_{peak}}{e} + k_2\right)^2}, \tag{10}$$

where I_{peak} is the peak current. Furthermore, approximations for large and small t_{peak} yield

$$I_{peak} = -k_1 \quad \text{(for large } t_{peak}\text{) and } I_{peak} = -\frac{k_3 e k_1}{e k_2^2 k_R - k_1} - k_1 \text{ (for small } t_{peak}\text{).} \tag{11}$$

Since the peak current is positive, $k_1 < 0$, and since, $k_2, k_3, e > 0$, I_{peak} is expected to be larger at a smaller t_{peak}. Additionally, from Figs. 4c and S1, it is clear that at larger scan rates, the current peak is achieved earlier, and the peak current is higher. Thus, the above model qualitatively explains the experimental observation.

This derivation assumes that mass-transfer limited ionic transport is the cause of the peak appearance. Hence, this proves that the mass-transfer limited ionic transport is the cause of the peak's appearance. This also explains the lower capacitance enhancement under UV illumination with the PVA/KCl gel electrolyte compared to the ionic liquid-based electrolyte (which does not exhibit peaks in the CV curves; thus, the ionic transport is not mass-transfer limited).

<u>Derivation explaining higher capacitance observed in GCD tests at higher currents for ionic liquid-based supercapacitors</u>

We assume the positive electrode-electrolyte interface to be at $x = 0$, and the negative electrode-electrolyte interface to be at $x = L$. The double-layer thicknesses at the positive and negative electrodes have been assumed to be DL_+ and DL_-, respectively.

Within the bulk electrolyte ($x = DL_+$ to $x = L - DL_-$)

$$\frac{\partial C_i}{\partial t} = D_i \frac{\partial^2 C_i}{\partial x^2} + \frac{z_i D_i F c_i}{RT} \frac{\partial^2 \emptyset}{\partial x^2} + \frac{z_i D_i F}{RT} \frac{\partial c_i}{\partial x} \frac{\partial \emptyset}{\partial x}, \tag{12}$$

$$\sum z_i c_i = 0, \tag{13}$$

where *i*= *c, a* with subscript *c* representing cations and *a* representing anions. In Eqs. 12 and 13, z represents charge number, D stands for diffusion coefficients, c stands for concentration, $\emptyset$ represents electrostatic potential, and F, R, and T are Faraday's constant, universal gas constant, and temperature, respectively. We assume that $z_c = 1,\ z_a = -1$.

While Eq. 12 relates the temporal derivative of concentration to the flux divergence, Eq. 13 represents the electroneutrality assumption within the bulk electrolyte.

Within the electric double layers at the positive ($x = 0$ to $x = DL_+$) and the negative ($x = L - DL_-$ to $x = L$) electrode-electrolyte interfaces, the ion transport is governed by the following equations:

$$\frac{\partial C_i}{\partial t} = D_i \frac{\partial^2 C_i}{\partial x^2} + \frac{z_i D_i F c_i}{RT} \frac{\partial^2 \emptyset}{\partial x^2} + \frac{z_i D_i F}{RT} \frac{\partial c_i}{\partial x} \frac{\partial \emptyset}{\partial x}\ , \tag{14}$$

$$\frac{\partial^2 \emptyset}{\partial x^2} = \frac{-F}{\varepsilon\varepsilon_0}\sum z_i c_i,$$

15

where ε is the relative dielectric constant of the electrolyte and ε_0 is the dielectric permittivity of vacuum. In the double layers, the electroneutrality condition (Eq. 13) is replaced by Poisson's law (Eq. 15). Assuming the voltage scan rate to be v V/s gives the following boundary conditions (Eqs. 16 and 17) for the electrostatic potential $\emptyset$,

$$\emptyset = E_i + \text{vt (forward scan)}, \ \emptyset = 0.8 - \text{vt (backward scan) at x=0}$$

16

and

$$\emptyset = 0 \text{ at x=}L.$$

17

Substituting Eq. 15 in Eq. 14 and assuming negligible cation concentration at the positive electrode-double layer interface, i.e., $c_c = 0$ at all times gives

$$\frac{\partial c_a}{\partial t} = D_a\frac{\partial^2 c_a}{\partial x^2} - \frac{D_a F^2 c_a^2}{RT\varepsilon\varepsilon_0} - \frac{D_a F}{RT}\frac{\partial c_a}{\partial x}\frac{\partial \emptyset}{\partial x} \ at \ x = 0$$

18

Similarly, assuming electroneutrality (Eq. 13) and negligible potential gradient at the double layer-bulk electrolyte interface ($x = DL_+, DL_-$) gives

$$\frac{\partial c_a}{\partial t} = 0 = \frac{\partial c_c}{\partial t} \ at \ x = DL_+, DL_-$$

19

This is a valid assumption because electroneutrality is valid within the bulk electrolyte. In supercapacitors, most potential gradient is present within the double layer, and we have negligible potential drop within the bulk electrolyte.

Moreover, current density I is given by

$$I = \sum z_i F\left(-D_i\frac{\partial C_i}{\partial x} - \frac{z_i D_i F C_i}{RT}\frac{\partial \emptyset}{\partial x}\right).$$

20

(a) Without illumination :

In case of no illumination, the externally recorded/supplied current is equal (in magnitude) to the current density due to the sum of the ionic fluxes (i.e., $J = I$, because of absence of any electron hole-pair generation and recombination as can be seen from Eq. 2).

For galvanostatic charge/discharge tests ($\frac{dI}{dt} = \frac{dJ}{dt} = 0$),

(i) <u>At the positive electrode-double layer interface</u> ($x = 0$) assuming $c_c = 0$ at all times gives

$$I = F\left(-D_c \frac{\partial c_c}{\partial x} + D_a \frac{\partial c_a}{\partial x} - \frac{F D_a c_a}{RT} \frac{\partial \emptyset}{\partial x}\right), \text{ at } x = 0 \text{ and}$$

21

$$0 = F\left[D_a \frac{\partial}{\partial x}\left(\frac{\partial c_a}{\partial t}\right) - F \frac{D_a}{RT}\left(\frac{\partial c_a}{\partial t}\frac{\partial \emptyset}{\partial x} + c_a \frac{\partial}{\partial x}\left(\frac{\partial \emptyset}{\partial t}\right)\right)\right] \text{ at } x = 0.$$

22

Order of magnitude analysis of Eq. 22, along with the assumption of $c_c = 0$ at x=0 gives

$$I \sim \frac{F D_a c_a}{SL_+}\left(1 - \frac{F\emptyset}{RT}\right) \text{ at } x = 0,$$

23

where SL_+ is the thickness of the Stern layer at the positive electrode-electrolyte interface. We assumed SL_+ to be the length scale instead of DL_+ because $c_c = 0$ is expected to be valid only very close to the positive electrode surface and not throughout the double layer. Extending the order of magnitude analysis to Eq. 22 and Eq. 14 and using condition 23 gives

$$\left(\frac{1 - \frac{F\emptyset}{RT}}{SL_+ c_a} - \frac{F^2 SL_+}{RT\varepsilon\varepsilon_0}\right)\frac{I}{F} \sim \frac{F\emptyset}{RTT_c}, \text{ at } x = 0,$$

24

where T_c is the charging time-scale.

Thus, the important terms that govern the supercapacitor response to galvanostatic charge-discharge tests are $I, SL_+, c_a, \varepsilon$. Now [1],

$$SL_+ \sim \frac{\varepsilon\varepsilon_0}{\sigma_{surf}}\left(\emptyset_{surf} - \varsigma\right),$$

25

where $\sigma_{surf}, \emptyset_{surf}$, and ς are the surface charge density on the electrode surface, electrostatic potential at the electrode surface ($x = 0$), and electrostatic potential at the Stern-layer diffuse layer interface within the double layer.

Thus, the Stern-layer thickness itself depends on electrode potential. Stern layer thickness has been shown to decrease with increasing concentration [1]. Moreover, surface anion concentration is expected to be proportional to σ_{surf}. Additionally, ε is largely expected to be independent of concentration [2].

Thus, although from condition 25, it may seem that the slope of potential versus time curve ($^{\emptyset}/_{T_c}$), should increase with increasing current density (which implies that charging time for the same voltage limits should decrease, which further implies lower capacitance (in most cases) at higher current densities); that need not always be the case because SL_+ itself depends on electrode potential.

The above analysis thus shows that higher capacitance at higher charging current densities may be possible under certain conditions, even though it is counter-intuitive and is not observed routinely.

<u>ii) At the negative electrode-double layer interface ($x = L$):</u> assuming $c_a = 0$ at all times gives

$$I = F\left(-D_c \frac{\partial c_c}{\partial x} + D_a \frac{\partial c_a}{\partial x} + \frac{F D_c c_c}{RT}\frac{\partial \emptyset}{\partial x}\right), \text{ at } x = L \text{ and} \tag{26}$$

$$0 = F\left[-D_c \frac{\partial}{\partial x}\left(\frac{\partial c_c}{\partial t}\right) + F\frac{D_c}{RT}\left(\frac{\partial c_c}{\partial t}\frac{\partial \emptyset}{\partial x} + c_c \frac{\partial}{\partial x}\left(\frac{\partial \emptyset}{\partial t}\right)\right)\right] \text{ at } x = L. \tag{27}$$

Order of magnitude analysis of Eq. 26, along with the assumption of $c_a = 0$ at x=L gives

$$I \sim -\frac{F D_c c_c}{SL_-} \text{ at } x = L, \tag{28}$$

where SL_- is the thickness of the Stern layer at the negative electrode-electrolyte interface. We assumed SL_- to be the length scale instead of DL_- because $c_a = 0$ is expected to be valid only very close to the negative electrode surface and not throughout the double layer. Thus, unlike the positive electrode, there does not seem to be a direct relation between the current density I and the negative electrode potential, which is always set to be 0.

(b) <u>With illumination:</u>

If the negative electrode is illuminated with UV light, then for the negative electrode, $|J| \neq |I|$, but for the positive electrode $G = R = 0$, so $|J| = |I|$. This implies that for galvanostatic charging, $\frac{dJ}{dt} = \frac{dI}{dt} = 0$ at the positive electrode- electrolyte interface. Thus, Eqs. 12- 25 would still be valid for explaining the unusual observation of higher capacitance at higher currents.

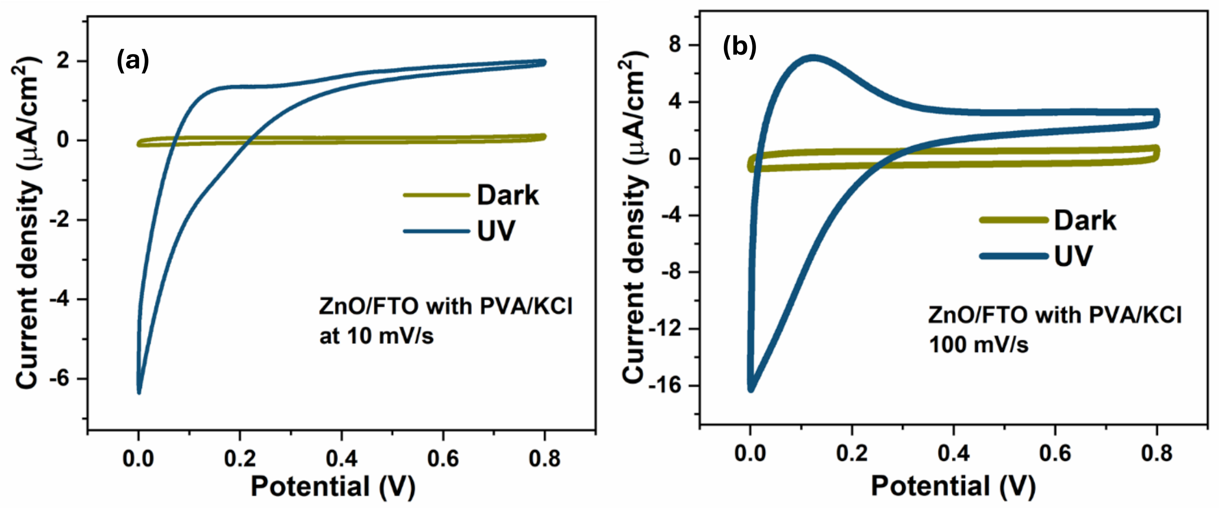

Figure S1: Cyclic Voltammograms of the solid-state symmetric supercapacitor using PVA/KCl gel electrolyte at (a) 10 mV/s and (b) 100 mV/s.

Table S1: Extracted parameters from EIS analysis.

Device	**R_s (Ohm)**	**R_{ct} (Ohm)**	**Q**
ZnO/FTO with PVA/KCl in Dark	152	-	$1.99*10^{-5}$
ZnO/FTO with PVA/KCl in UV	54.92	-	$4.97*10^{-4}$
ZnO/FTO with BMIM-BF_4 in Dark	28.54	3.28 (Exp.)	$1.29*10^{-5}$
ZnO/FTO with BMIM-BF_4 in UV	25.58	4.78 (Exp)	$2.44*10^{-4}$

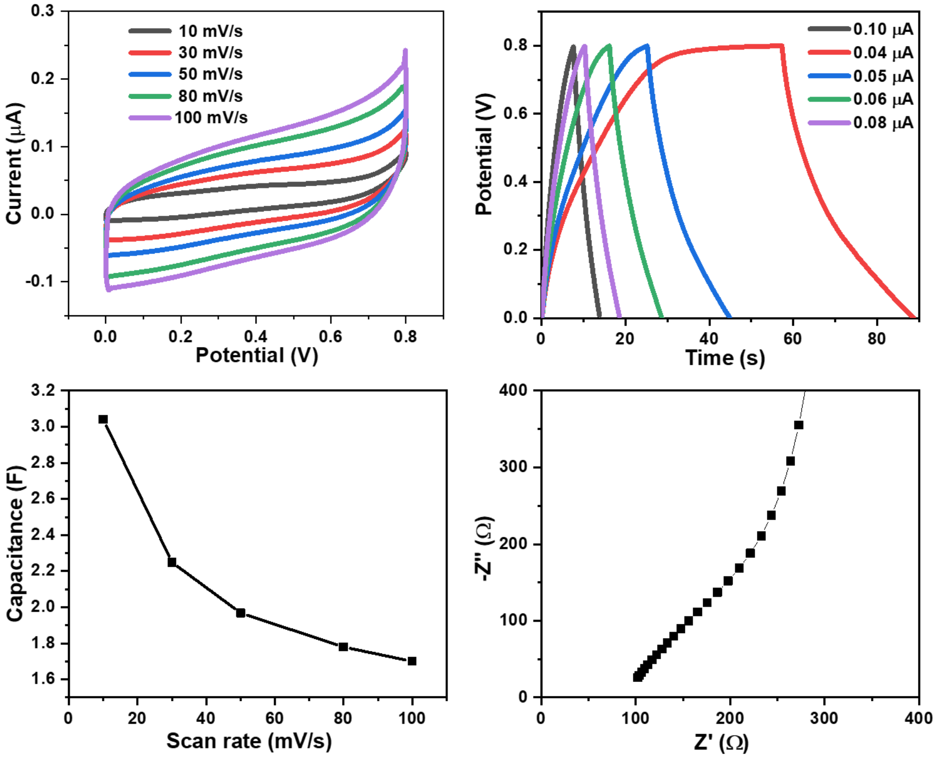

Figure S2: (a) CV, (b) GCD analysis, (c) Capacitance corresponding to the CV, and (d) Nyquist plot for BMIM-BF4 electrolyte.

References

[1] M. A. Brown, A. Goel, and Z. Abbas, "Effect of Electrolyte Concentration on the Stern Layer Thickness at a Charged Interface," *Angew. Chemie Int. Ed.*, vol. 55, no. 11, pp. 3790–3794, Mar. 2016.

[2] X. Wang, K. Liu, and J. Wu, "Demystifying the Stern layer at a metal-electrolyte interface: Local dielectric constant, specific ion adsorption, and partial charge transfer," *J. Chem. Phys.*, vol. 154, no. 12, p. 124701, Mar. 2021.